Oxidation of Metals, Vol. 22, Nos. 5/6, 1984

Platinum and the Oxidation Behavior of a Nickel Based Superalloy

G. J. Tatlock* and T. J. Hurd*

Received April 23, 1984

The oxidation behavior in air of a platinum containing nickel based superalloy (RJM2012) is compared with that of a similar alloy (IN792+Hf) without platinum. The distinct improvement in the oxidation resistance of the platinum containing alloy at high temperatures (1100°C) is explained in terms of the oxide morphologies and oxidation kinetics. In particular, it appears that platinum has a small but significant effect on the diffusion of other species in the alloy, and a model is presented to account for the complex sequence of oxide development, which culminates in the formation of a protective alumina scale.

KEY WORDS: platinum; nickel-based superalloy; oxidation; RJM2012, IN792+Hf.

INTRODUCTION

Investigations of the oxidation behavior of Ni-Pt alloys were first carried out some 35 years ago by Kubaschewski and von Goldbeck,[1] but it is only recently that Pt has been added to nickel based superalloys to improve their oxidation resistance, either in the form of a coating[2] or incorporated into the base alloy.[3] Pt-Al coatings were first developed during a search for diffusion barriers to retard the diffusion of aluminum from a coating into the bulk alloy, but subsequent work (e.g., Jackson and Rairden[4]) has shown that the Pt remains concentrated at the surface of the sample after aluminization and acts as a diffusion medium for the aluminum rather than a barrier.

*Dept. of Metallurgy and Materials Science, University of Liverpool, P.O. Box 147, Liverpool L69 3BX, U.K.

0030-770X/84/1200-0201$03.50/0

The incorporation of platinum into α-Al_2O_3 scales and their subsequent adhesion has been studied by several groups (e.g., Felten,[5] Felten and Pettit,[6] and Fountain *et al.*[7]), but few systematic attempts have been made to investigate the microstructures which form when platinum is added to super-alloys. Felten[5] carried out studies of additions to the Ni-8Cr-6Al system and showed that both Pt and Rh enhance oxide adherence at 1100 and 1200°C. It appeared that platinum allowed the Al_2O_3 scale to reform when modest spalling had occurred, although a detailed mechanism was not presented. Coupland *et al.*[8] have also shown that a platinum containing superalloy designated RJM2012 gives much better cyclic oxidation behavior than a similar alloy without platinum (IN792+Hf) and that the hot corrosion resistance is also improved with Pt additions. At Liverpool we have been investigating the microstructures of both oxidized and hot corroded samples of RJM2012 and IN792+Hf; herein we present our oxidation results.

EXPERIMENTAL PROCEDURE

The major part of this investigation was concerned with two nickel based superalloys, IN792+Hf and the platinum containing RJM2012. Their compositions are given in Table I. The two alloys are similar in composition with the exception of 4.5% Pt substituted for some of the nickel in IN792+Hf. After casting, both alloys were given a standard, three stage heat treatment of 4 hr at 1120°C, 8 hr at 920°C, and finally 16 hr at 760°C in a vacuum of $\sim 10^{-3}$ torr with air cooling between each stage. Coupons $10 \times 10 \times 5$ mm were cut from the centers of the ingots and abraded on SiC paper with a final finish at 600 grit followed by washing and degreasing before oxidation trials.

Most of the oxidation runs were carried out in air at 900 and 1100°C in a horizontal furnace. Although the testing was primarily isothermal, some temperature cycling was imposed by the removal of samples from the furnace for examination about every 20 hr up to 100 hr and every 100 hr up to 600 hr. The surface scales and cross-sections through the metal oxide interfaces

Table 1. Alloy Compositions in Weight Percent

Element	Ni	Cr	Co	Ti	Ta	Al	Mo	W	Hf	Pt	C	B	Zr
IN792+Hf	Bal.	12.52	9.00	4.14	3.95	3.51	2.02	4.01	0.88	—	0.13	0.015	0.11
RJM 2012	Bal.	12.08	9.27	3.77	3.49	3.42	1.72	2.98	0.75	4.70	0.09	0.015	0.02

were examined on a JX50A electron probe microanalyzer and a Philips 501 SEM equipped with an EDAX energy dispersive X-ray analysis system. Higher spatial resolution investigations were also carried out on thinned sections in a Philips 400T TEM. In this case sections were cut perpendicular to the metal-oxide interface and mechanically thinned. Electron transparent regions round the metal-oxide interface were then produced by ion beam thinning the samples after the method described by Manning and Rowlands.[10]

RESULTS

The cyclic oxidation behavior of RJM2012 and IN792 has previously been investigated by Coupland *et al.*[8], and their results of weight change with number of cycles are reproduced in Figs. 1 and 2. At 900 and 1000°C both alloys exhibit a similar change in weight. The picture is very different at 1100°C, however, where the weight loss due to spalling is much reduced in RJM2012 compared with IN792. Microstructural studies were therefore

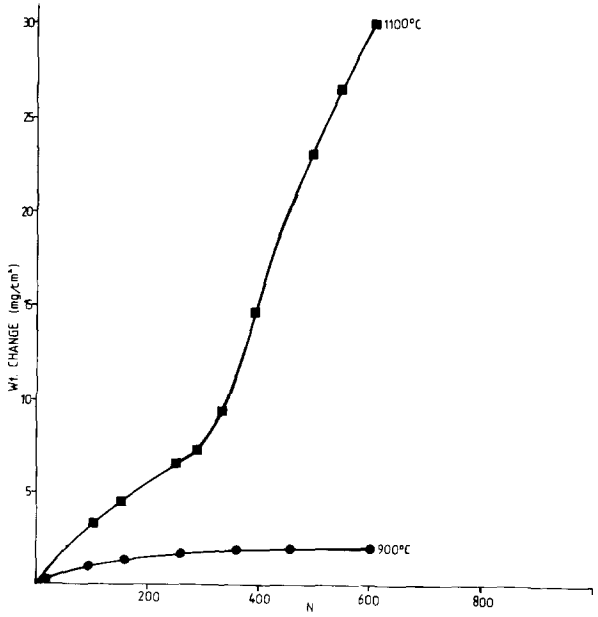

Fig. 1. Cyclic oxidation data for IN792 + Hf after Coupland *et al.*[8]

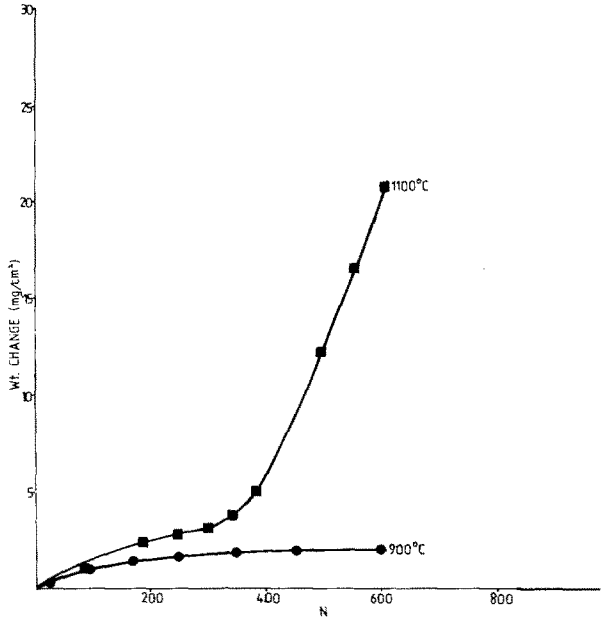

Fig. 2. Cyclic oxidation data for RJM2012 after Coupland *et al.*[8]

carried out on the two alloys after oxidation at 900 and 1100°C, and the results can be summarized as follows:

Scale Morphologies

IN792+Hf at 900°C

Investigation of the scales formed on IN792 showed that they consisted of a chromium-titanium rich outer scale on top of an aluminum rich layer (Fig. 3). Although the scale is reasonably uniform, initially, after only 40 hr some cracking and spalling is observed (Fig. 4). The aluminum rich layer left after spalling is rather smooth and protective although further spalling is seen after longer times.

RJM2012 at 900°C

The oxide morphology is similar to that of IN792 at 900°C (Fig. 5). The presence of titanium rich needles on the surface is more pronounced at early times, and the chromium rich scale is more convoluted and spalls very readily after the first few hours under test (Fig. 6). Hence at 900°C, RJM2012 appears to be more prone to spalling and the scale is less protective than that formed on IN792.

Fig. 3. IN792+Hf outer scale after oxidation for 20 hr at 900°C.

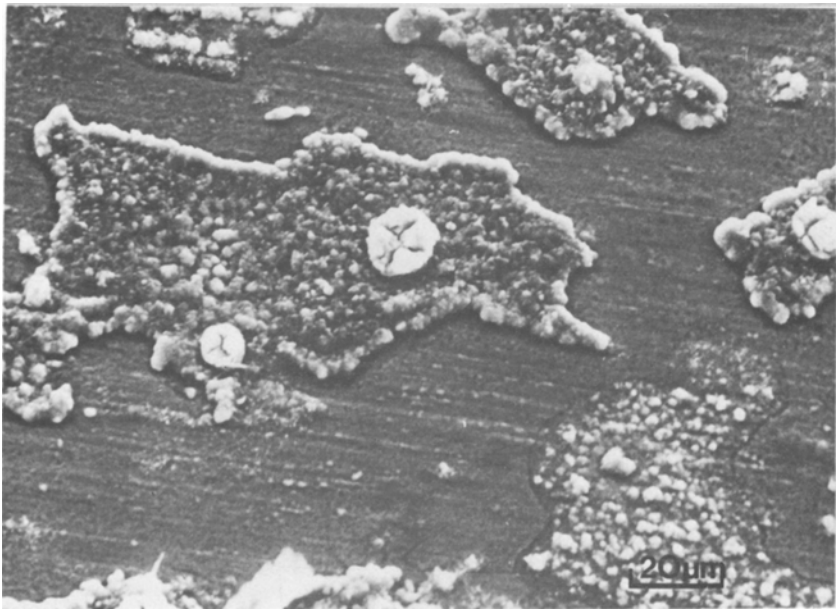

Fig. 4. IN792+Hf outer scale after oxidation for 60 hr at 900°C.

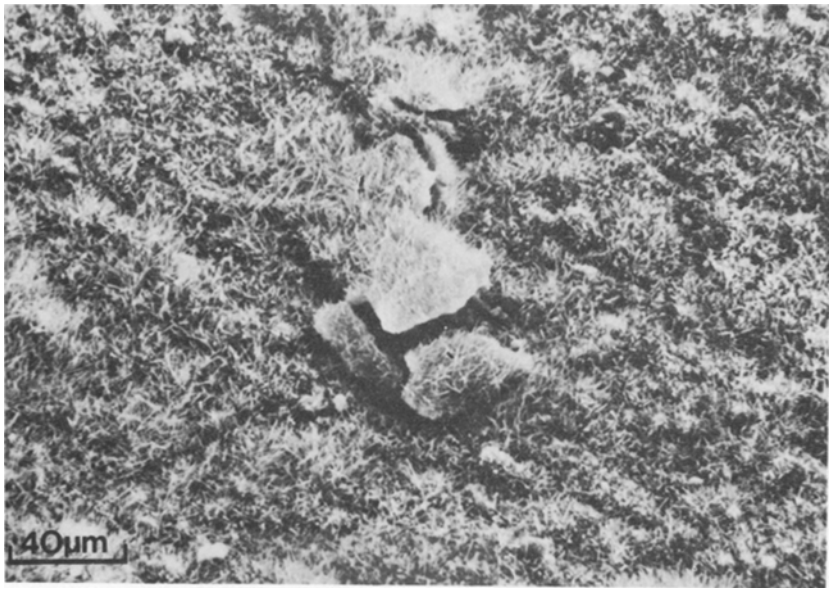

Fig. 5. RJM2012 outer scale after oxidation for 20 hr at 900°C.

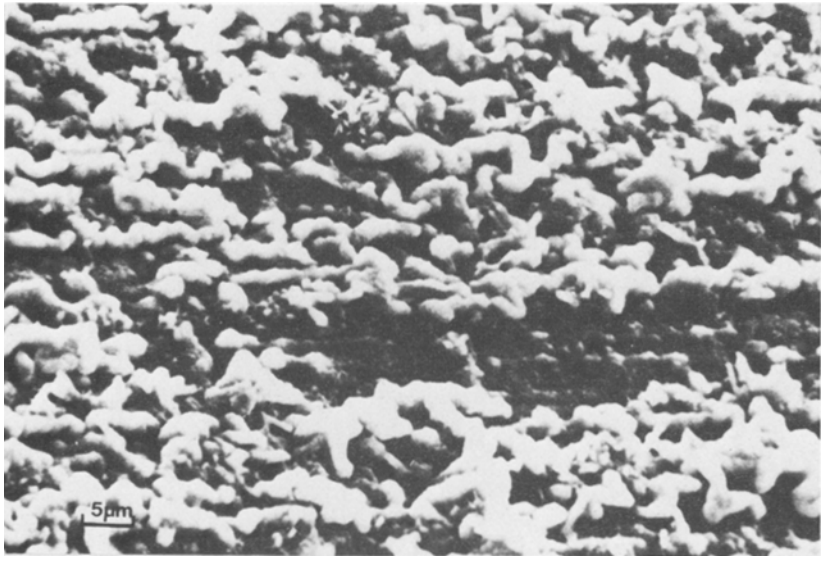

Fig. 6. RJM2012 outer scale after oxidation for 60 hr at 900°C.

IN792+Hf at 1100°C

The behavior of each of the two alloys is rather different at 1100°C. Up to 100 hr the scales formed on IN792+Hf were quite protective with little evidence of spalling (Fig. 7). However, at longer times the scale broke down and a large number of isolated oxide flakes formed (Fig. 8). The spalled regions did not "heal," and after much longer times (~400 hr), angular nickel rich oxide was present over the majority of the surface (Fig. 9).

Cross-sections through the scales together with elemental X-ray mapping gave a clearer picture of the sequence of events. Figure 10, for example, shows a secondary electron image and elemental maps through a sample after 500 hr at 1100°C. The internal aluminum rich oxides were very prominent while the outer scale contained large amounts of chromium, nickel, and titanium. Tantalum also segregated to the area immediately below the outer scale. The crucial point, however, was that the internal aluminum did not form a continuous band, and spalling of the outer scale produced a fresh attack of the metal with new internal oxides being formed.

RJM2012 at 1100°C

The sequence of events was rather different in RJM2012. The oxide scale on this alloy was already badly spalled after only 40 hr on test (Fig. 11),

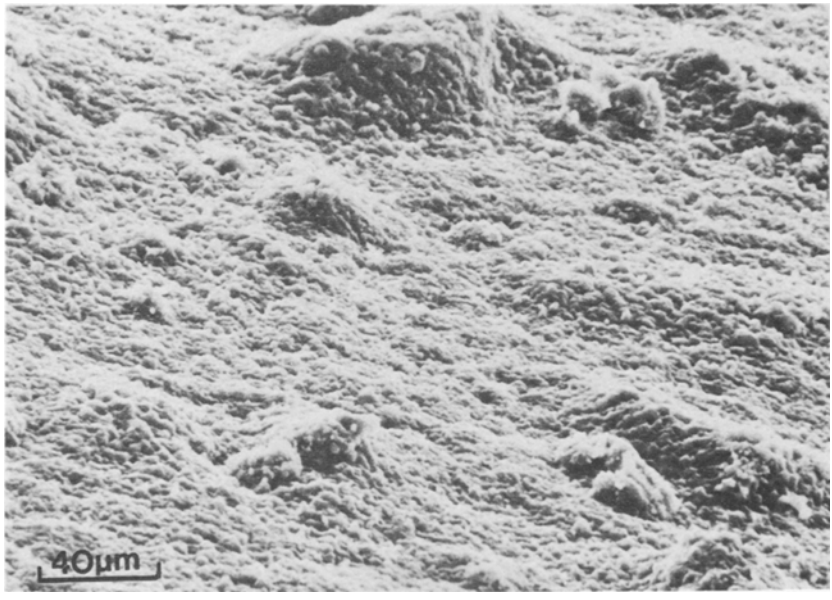

Fig. 7. IN792+Hf outer scale after oxidation for 20 hr at 1100°C.

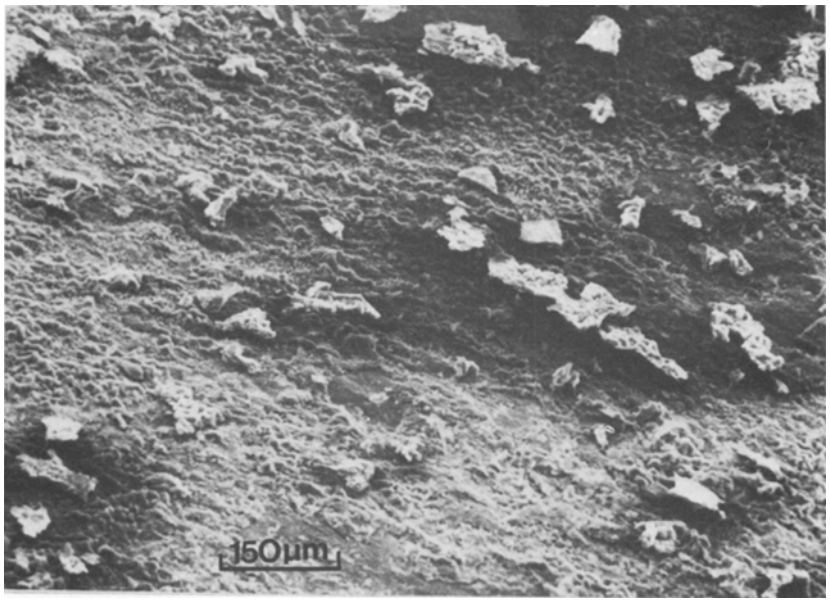

Fig. 8. IN792+Hf outer scale after oxidation for 150 hr at 1100°C.

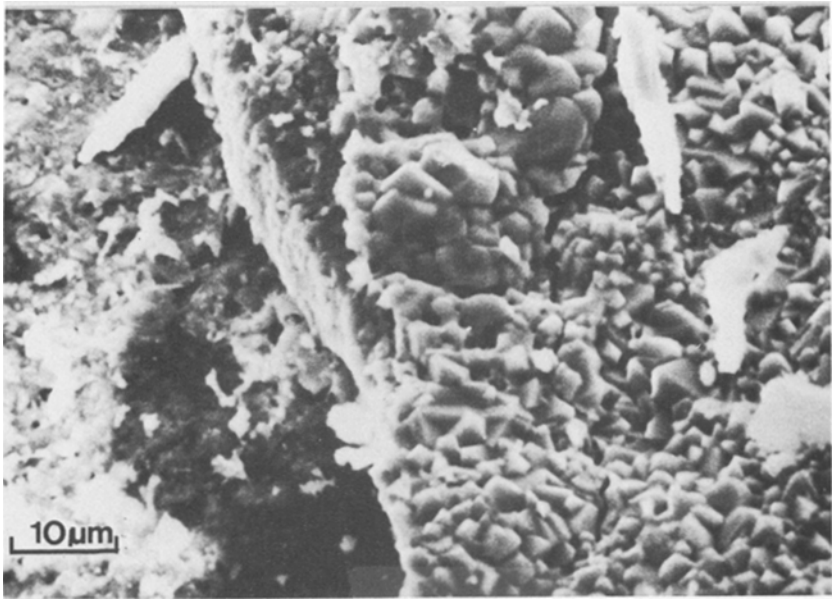

Fig. 9. IN792+Hf outer scale after oxidation for 400 hr at 1100°C.

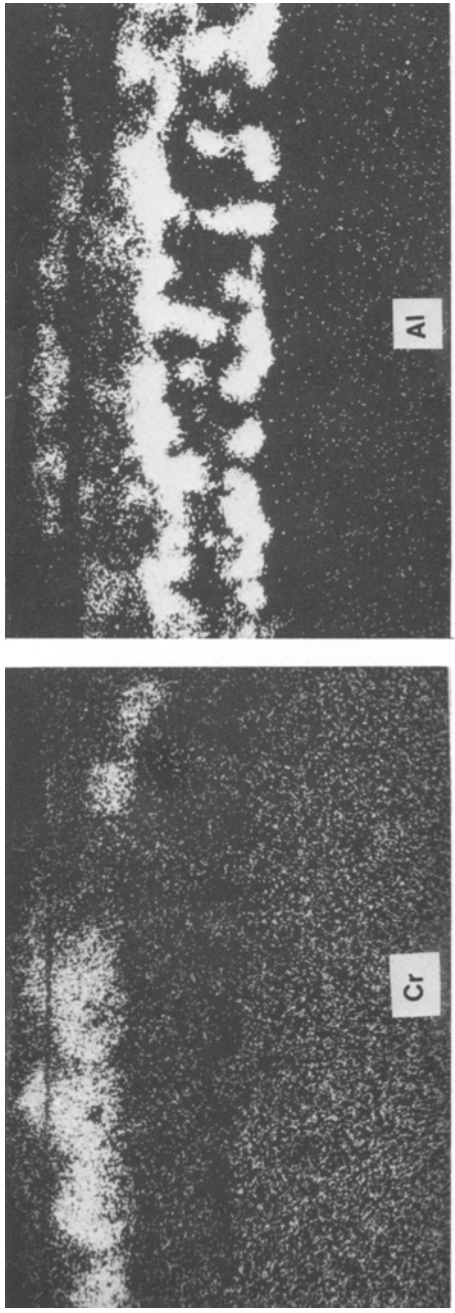

Fig. 10. SEI and elemental maps of cross-section through oxide scale on IN792+Hf after 500 hr at 1100°C.

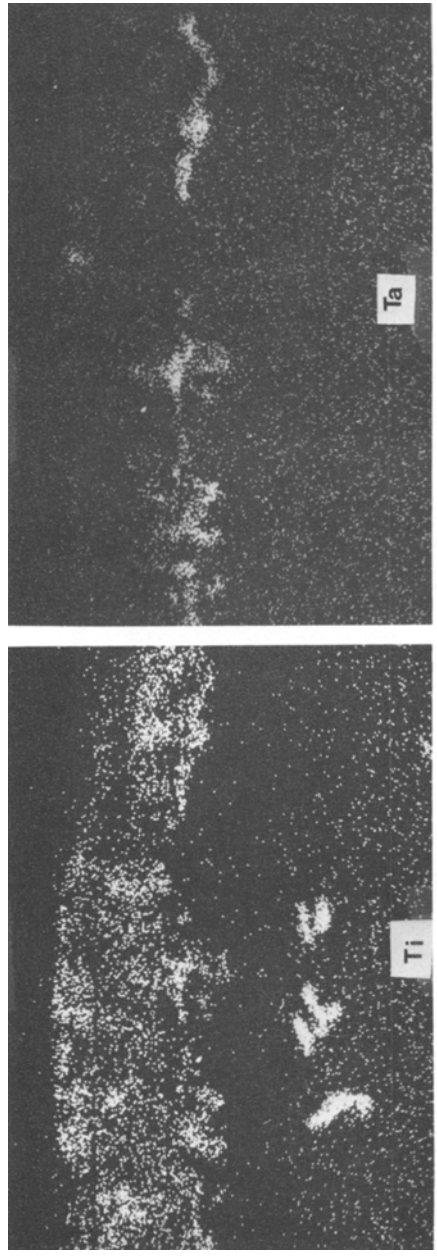

Fig. 10. Continued.

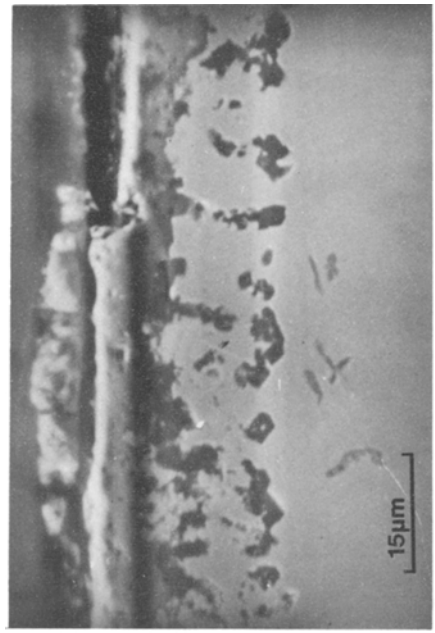

f

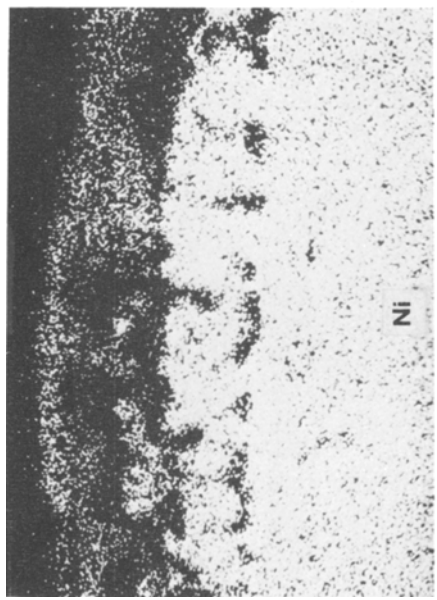

e

Fig. 10. Continued.

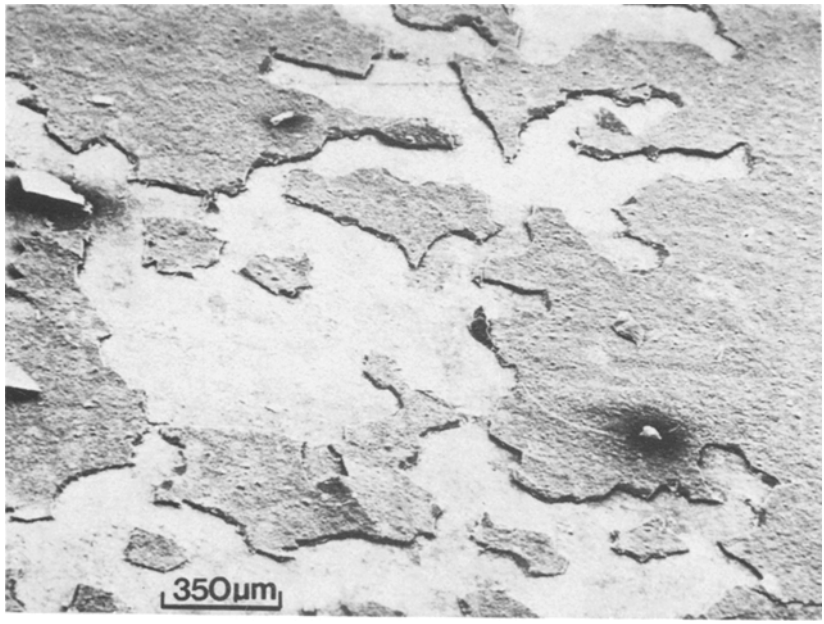

Fig. 11. RJM2012 outer scale after oxidation for 40 hr at 1100°C.

although the scale still consisted of a titanium rich outer region over a chromium rich layer with tantalum present near the base of the scale. However, in contrast to the lower temperature observations, the titanium was not present as needles. The areas beneath the spalled scale were still aluminum rich, although large amounts of Pt, together with some Cr and Ni, were present. After 100 hr most of the original scale had spalled away, and after 200 hr the morphology of the outer surface had changed to an almost continuous layer of alumina. Pt particles were found on this layer together with a few areas of Cr rich oxide (Fig. 12). Very little further change was observed even after 600 hr testing. The alumina remained adherent with no sign of spalling or cracking. However, the Pt particles were no longer present, and small mounds of angular nickel rich oxide were growing through the few chromium rich regions which were still present (Fig. 13).

Once again cross-sections through the scales together with elemental X-ray maps gave further insight into the oxide formation. Figure 14 shows the secondary electron image and X-ray maps for RJM2012 after 500 hr oxidation at 1100°C. The bulk of the surface consisted of a continuous alumina film with no internal aluminum oxides. The internal oxides which were present at earlier times, however (e.g., 30 hr; see Fig. 15) appeared to

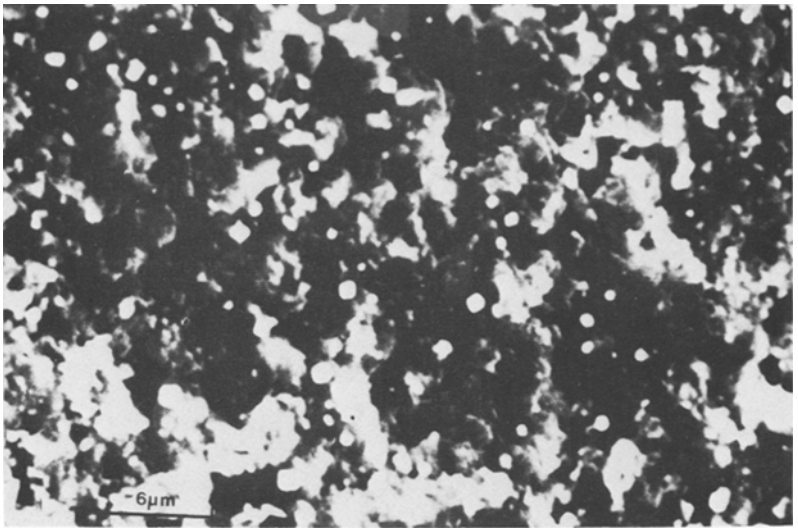

Fig. 12. RJM2012 outer scale after oxidation for 100 hr at 1100°C.

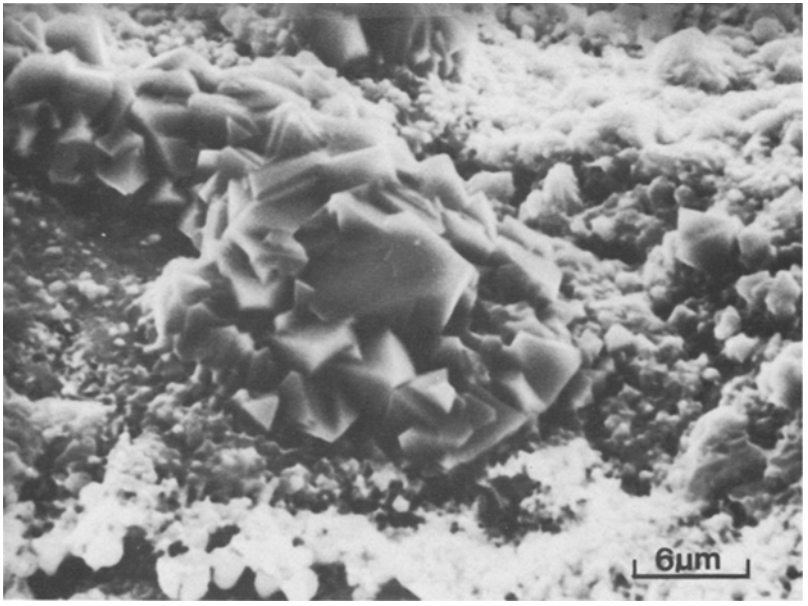

Fig. 13. RJM2012 outer scale after oxidation for 600 hr at 1100°C.

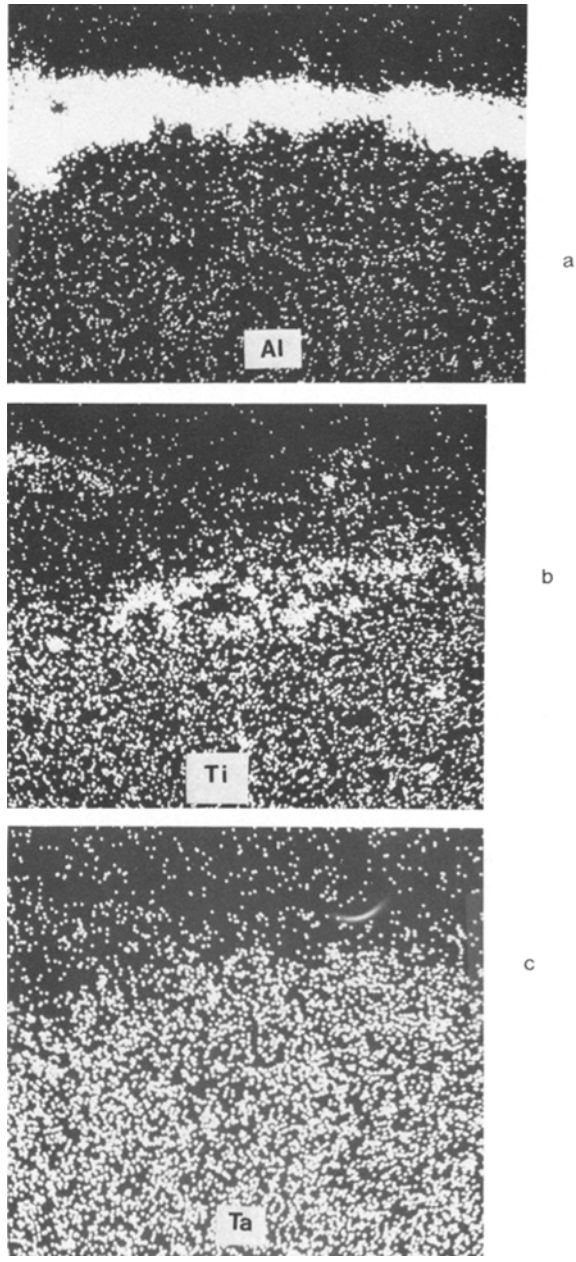

Fig. 14. SEI and elemental maps of C/S through RJM2012 after 500 hr at 1100°C.

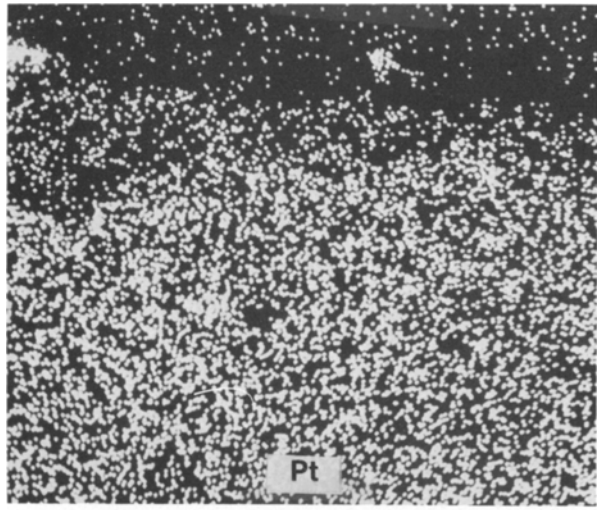

d

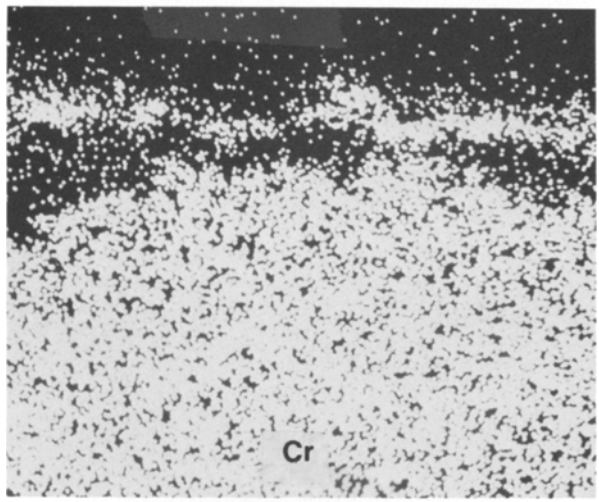

e

Fig. 14. Continued.

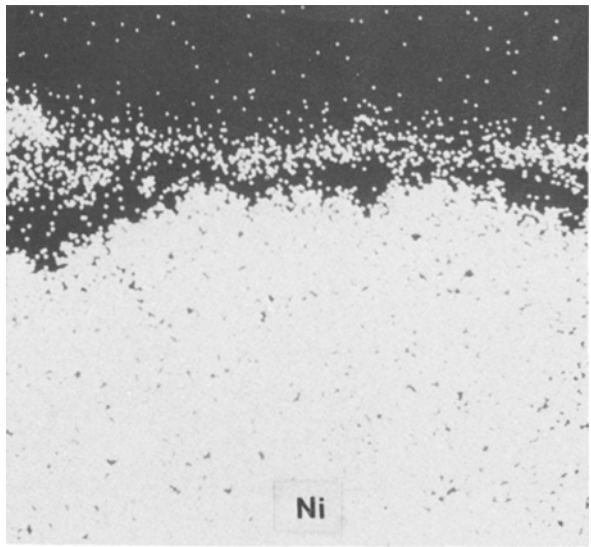

f

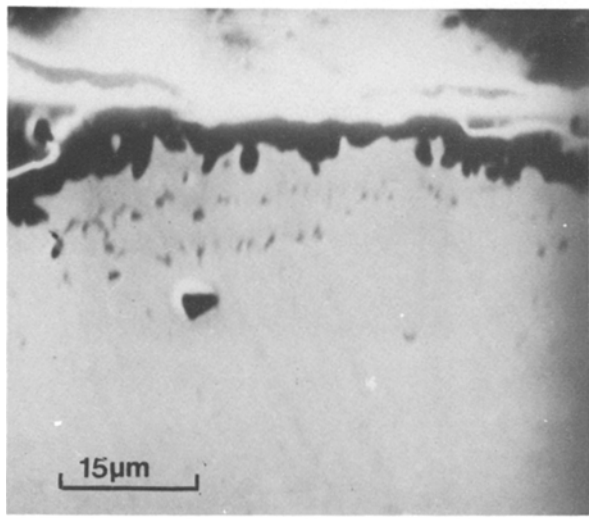

g

Fig. 14. Continued.

have grown and joined together to form a continuous film, and this appeared to be the crucial step in the corrosion protection.

Elemental Profiles

The competition between the formation of external scales and internal oxides has been well documented[11] and is principally governed by the amounts and diffusion of aluminum and oxygen through the alloy. In order to investigate further the high temperature behavior of RJM2012 and IN792+Hf, elemental profiles were recorded across sections through the metal-oxide interfaces, and the amounts of the major elements were recorded after different oxidation times. A typical series of profiles for RJM2012 and IN792+Hf are shown after 20 hr oxidation (Fig. 16) and 92 hr oxidation

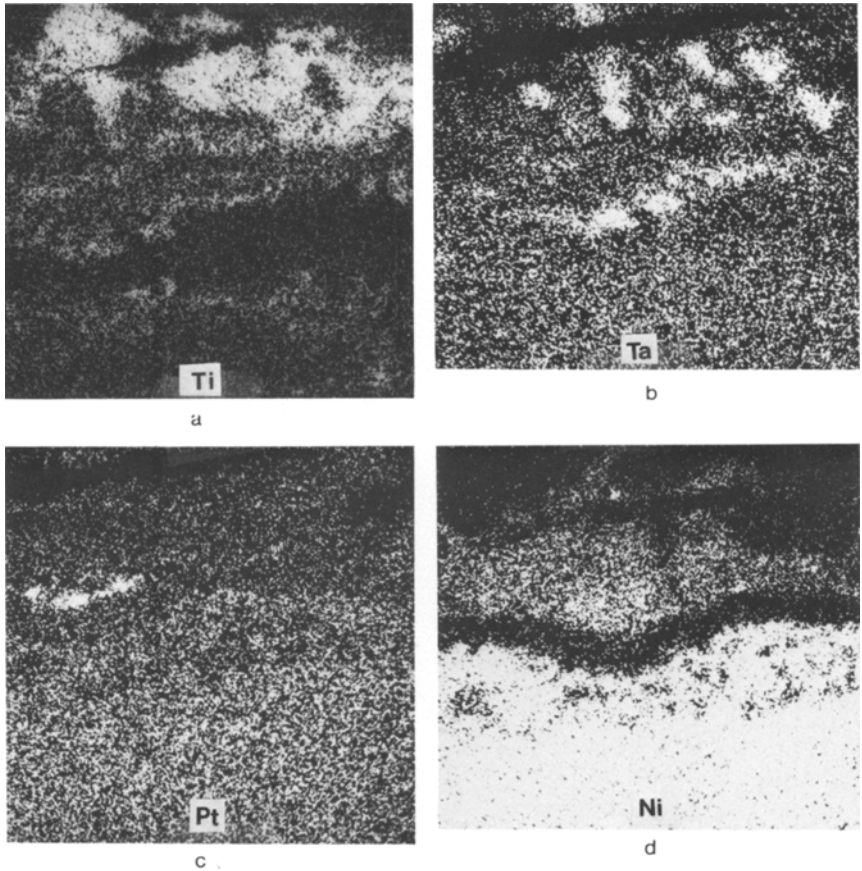

Fig. 15. SEI and elemental maps of C/S through RJM2012 after 30 hr at 1100°C.

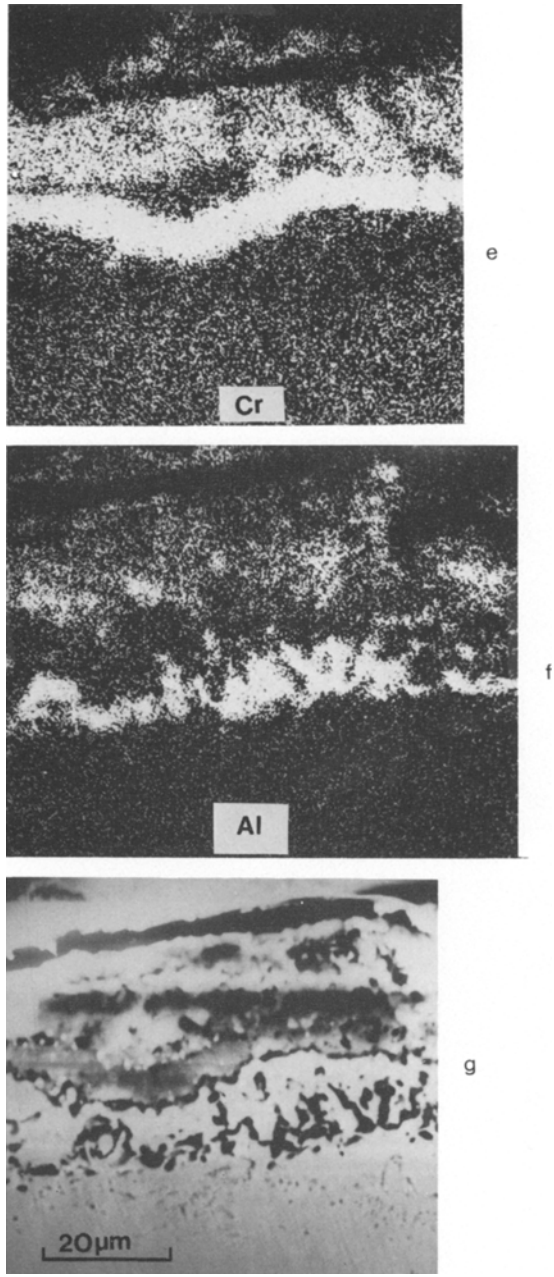

Fig. 15. Continued.

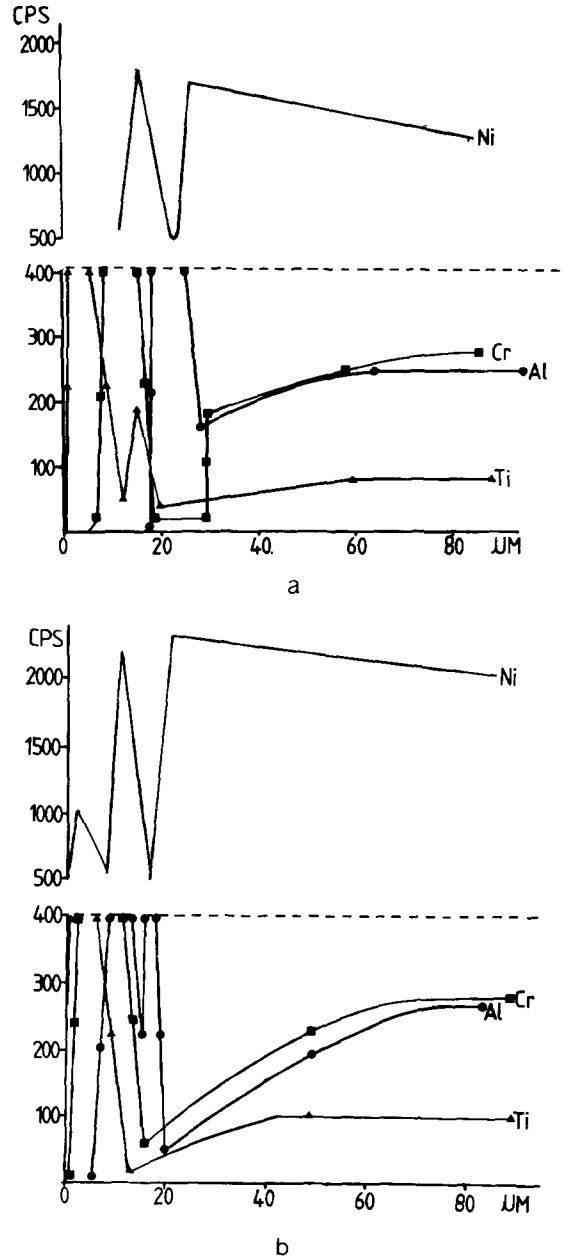

Fig. 16. Elemental profiles across sections through the alloys after 20 hr oxidation. (a) RJM2012; (b) IN792+ Hf.

(Fig. 17). The peaks in the Al, Cr signals are artificially truncated due to the method of data collection, and their height has no physical significance. What does show up clearly, however, is the degree of segregation of the various elements with time, and in particular, the level of depletion of Al and chromium below the oxide scale and internal oxides. Since the formation of an alumina film appears to be the most critical step, the degree of Al depletion was investigated further. Figure 18 shows a plot of the amount of aluminum just below the alumina layer vs. time. The value was normalized by dividing the measurements by the aluminum signal from the bulk alloy. The curves for the two alloys are significantly different, and this will be returned to later in the discussion.

Although the profiles suggested that the oxide developed under a diffusion controlled mechanism, some higher resolution work was also done on thin transmission samples containing the metal oxide interface. The scales under examination were rather thin (Fig. 19), and hence sample preparation was difficult. Nothing untoward was observed at the interfaces, however, with the exception of Hf rich particles in the oxides. Voiding was also observed along the oxide grain boundaries in some cases but not at the metal oxide interface in RJM2012.

Model Alloys

In order to further investigate the interaction between the different elements in the alloys, some simpler model alloys were also produced and tested. In each case the elemental constituents were melted in an argon arc furnace into a button ~20 mm diam, which was then homogenized at 1000°C for 24 hr under argon. Two series of alloys were produced. The first included Ni-3% Al, Ni-6% Al, and Ni-9% Al; in the corresponding set, $4\frac{1}{2}$% Pt was substituted for some of the nickel. The second contained Ni-12% Cr-6% Al and Ni-12% Cr-6% Al-$4\frac{1}{2}$% Pt.

The Ni-Al system has been studied extensively by Pettit,[11] who showed that the formation of external scales and internal oxides depends critically on the aluminum concentration in the alloy; the overall mechanisms have been reviewed by several authors (e.g., by Wallwork[12]). The present experiments confirmed the data shown by Pettit, since the Ni-3% Al and Ni-6% Al samples both formed internal oxides (see, for example, Fig. 20), while the Ni-9% Al formed an external scale. If Pt is added to the alloy, then any major change in the aluminum diffusion rate might change the balance: for example, the Ni-6% Al-$4\frac{1}{2}$% Pt alloys might then form an external scale. In practice this was not observed (Fig. 21), and internal alumina formed in a similar way to the non-Pt containing alloy.

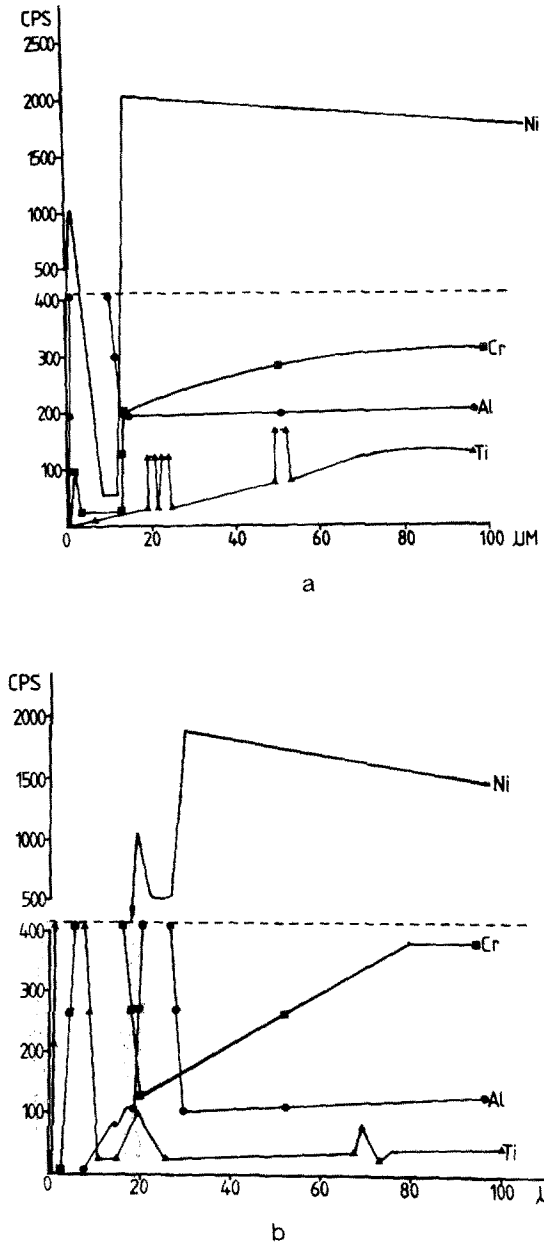

Fig. 17. Elemental profiles across sections through the alloys after 92 hr oxidation. (a) RJM2012; (b) IN792+Hf.

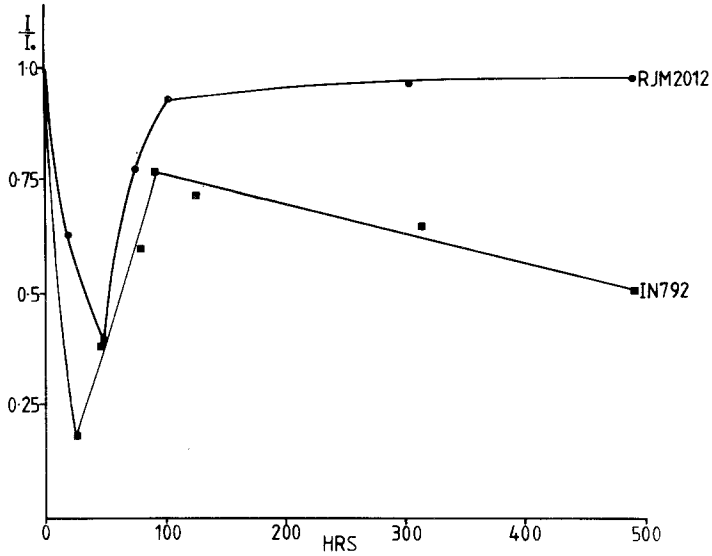

Fig. 18. Plot of aluminum level below the internal oxides against time. The lines only emphasize the trends.

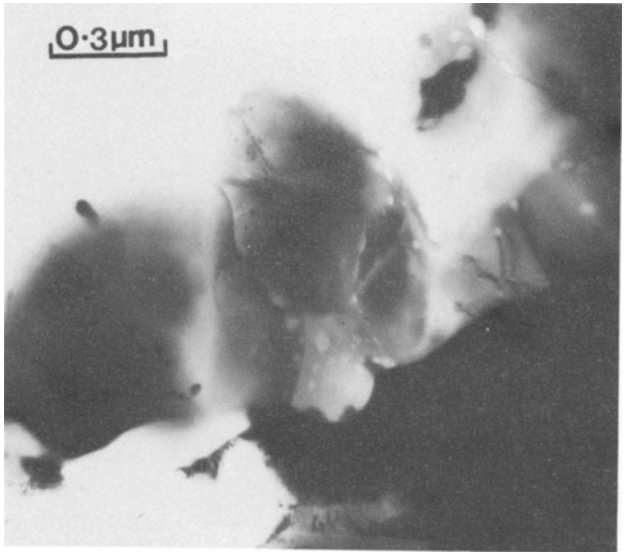

Fig. 19. TEM image of metal/oxide interface in RJM2012.

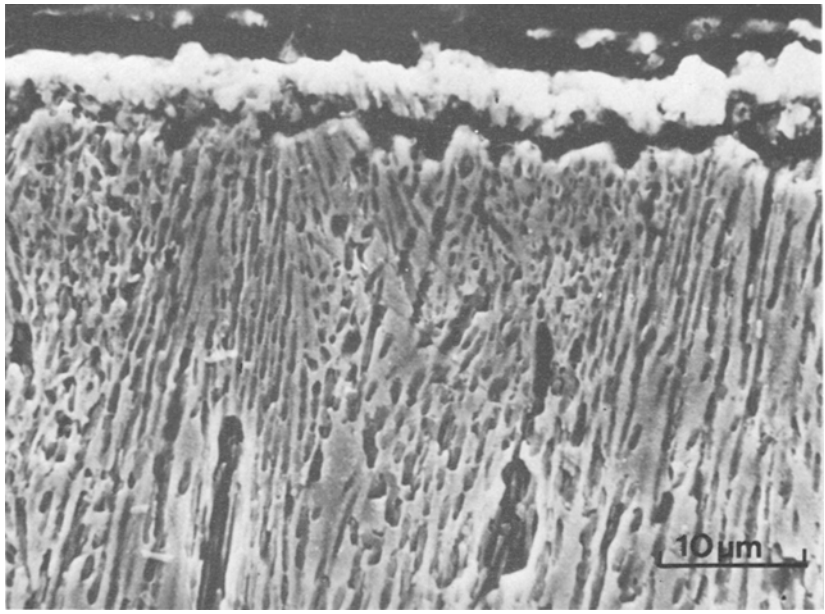

Fig. 20. Cross-section through a Ni-6% Al alloy oxidized at 1100°C showing extensive internal oxidation.

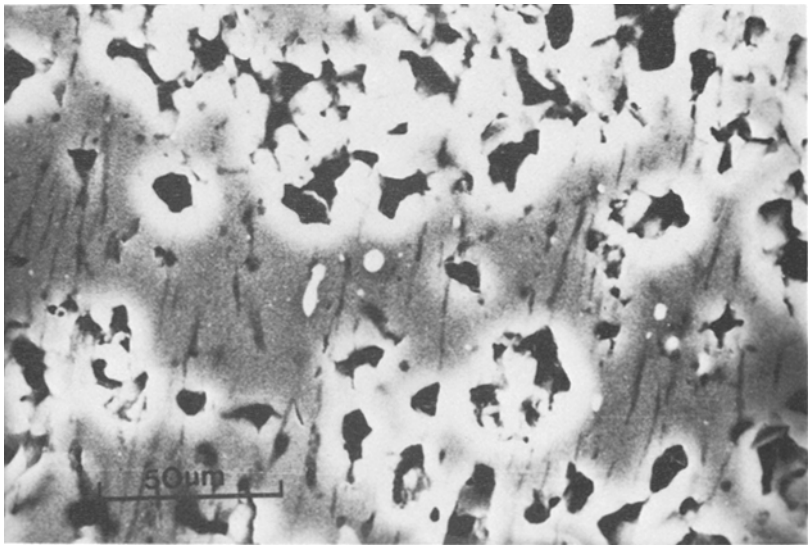

Fig. 21. Cross-section through a Ni-6% Al-4½% Pt alloy oxidized at 1100°C showing internal oxidation and Pt particles.

Major effects which were observed, however, include the segregation of the Pt to the region below the external scale and the presence of Pt particles within the NiO scale. These implied that the Pt was driven out from the oxide scale and was enriched within the subscale region. Individual precipitates could also be found in the oxide. It is thought that such precipitation may explain the presence of Pt particles in the RJM2012 samples, and we discuss this further below. The formation of internal aluminum oxide depends on the diffusion of both oxygen and aluminum. Hence if the oxygen is supplied very rapidly, then a slight change in the aluminum diffusion rate would not have much effect.

In the presence of a more protective external scale, for example, chromia, the oxygen diffusion would be slowed, and platinum may have a bigger influence. Hence experiments were also conducted on a Ni-12% Cr-6% Al-$4\frac{1}{2}$% Pt alloy. The results varied somewhat from place to place across the sample, suggesting a composition at a transition stage, but where a chromia rich scale had been established (Fig. 22), analysis of the cross-section showed a nickel rich surface on a chromia rich scale, with a continuous layer of alumina at the base of the scale. There was no evidence of any internal oxidation, but Pt rich particles were once more observed in the region of the chromia/alumina interface, just as in the case of RJM2012.

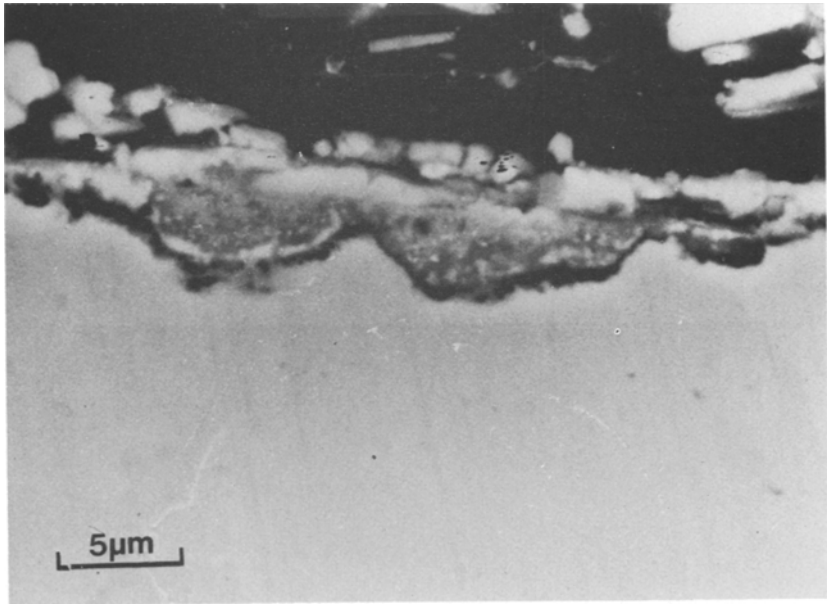

Fig. 22. Cross-section through a Ni-12% Cr-6% Al-$4\frac{1}{2}$% Pt alloy oxidized at 800°C showing Pt particles in the region of the chromia/alumina interface.

DISCUSSION

The kinetic studies showed that RJM2012 and IN792+Hf behaved in similar ways at 900°C but very differently at 1100°C, and this was largely borne out by the morphological studies. The platinum appeared to promote major changes in the scale development at 1100°C, and hence the main questions which need addressing are what happens to the platinum at this temperature and how does it influence the formation of the alumina layer.

The first question may be answered by comparing the results in RJM2012 with those in the model alloys. In the case of the Ni-Al-Pt alloys, Pt is both precipitated out in the nickel oxide and increased in concentration in the matrix below the scale. This latter effect is not observed in either RJM2012 or in the Ni-Cr-Al-Pt alloy, suggesting that the internal alumina in the more complex, Cr containing alloys coalesces into a continuous layer before the oxides closer to the surface have completely formed. Hence the platinum, which is relatively insoluble in the oxide, is swept inwards until it meets the alumina barrier and forms precipitates in the region of the chromia/alumina interface. Therefore the presence of the platinum particles is a result of the changes in oxidation mechanism rather than its cause.

The crucial difference between oxide formation in RJM2012 and IN792+Hf at 1100°C appears to be the formation of a continuous alumina layer from the band of internal oxide. The formation of any internal oxide relies on a balance between the inward diffusion of oxygen and the outward diffusion of aluminum. This can be characterized to some extent by the aluminum level at the base of the internal oxide, as illustrated in Fig. 18. The curves for both alloys show the same trend with a rapid initial depletion followed by a slow recovery to an equilibrium value, as the growth of the chromia and alumina scales gradually cuts down the oxygen diffusion. In the case of IN792+Hf, the aluminum level never reaches a value sufficiently high to produce a continuous alumina film before the combined oxygen and aluminum levels below the internal oxide layer induce new internal oxide growth. A continuous alumina film is formed on RJM2012, however, and the decrease in oxygen diffusion eventually allows the aluminum level to return to the bulk value immediately below the scale.

This subtle mechanism appears to be reproduced in the model alloy of Ni-Cr-Al-Pt. Hence it would seem that the platinum containing alloy acts as a medium for the rapid diffusion of aluminum, and a small change in the kinetics is enough to produce a large change in overall oxidation behavior. Alternatively, the platinum could be influencing the diffusion of oxygen through the chromium rich outer scale, slowing it down sufficiently to allow the alumina level to increase without the formation of internal oxides. Several authors have also suggested that Pt additions may improve the adherence of alumina scales.[5,13,14] This could be an additional benefit

in the present case since there is little point in designing an alloy to produce a continuous alumina scale if it spalls readily under cyclic thermal testing.

CONCLUSIONS

The oxidation rates are similar for RJM2012 and IN792+Hf at 900°C but very different at 1100°C. These differences are evident in cross-sections through the scales which highlight the protective role of an alumina film formed by the growth of internal oxide precipitates in RJM2012 at 1100°C. The internal oxides in IN792+Hf do not join up in this way; hence the alloy is continuously attacked, and new internal oxides are formed. It is suggested that the most likely reasons for this difference are associated with the influence of platinum on the aluminum diffusion, where the subscale aluminum level builds up sufficiently rapidly to inhibit further internal oxide growth. Alternatively, the doping of oxides in the outer scale with platinum may slow the oxygen diffusion through this scale and allow the aluminum level to build up before further internal oxides are formed. Further work is in progress to test these mechanisms.

What is clear, however, is that small changes in critical concentrations have a major effect on the performance of the alloys. The influence of platinum on the hot corrosion of the alloys is rather different and will be the subject of a future paper.[9]

ACKNOWLEDGMENTS

The financial support of SERC and Johnson Matthey Research Center are gratefully acknowledged, together with useful discussions with Drs. D. R. Coupland, I. R. McGill, and N. Swindells.

REFERENCES

1. O. Kubaschewski and O. von Goldbeck, *J. Inst. Met.* **76**, 255 (1949).
2. G. Lehnert and H. W. Meinhardt, *Electrodepos. Surface Treat.* **1**, 189 (1972/73).
3. D. R. Coupland, C. W. Corti, and G. L. Selman, *Proc. Int. Conf. Behavior of High Temp. Alloys in Aggressive Environments* (Metals Society, London, 1980), p. 525.
4. M. R. Jackson and T. R. Rairden, *Met. Trans.* **8a**, 1697 (1977).
5. E. J. Felten, *Oxid. Met.* **10**, 23 (1976).
6. E. J. Felten and F. S. Pettit, *Oxid. Met.* **10**, 189 (1976).
7. J. G. Fountain, F. A. Golightly, F. H. Stott, and G. C. Wood, *Oxid. Met.* **10**, 341 (1976).
8. D. R. Coupland, C. W. Hall, and I. R. McGill, *Plat. Met. Rev.* **26**, 2 (1982).
9. T. J. Hurd and G. J. Tatlock, to be published.
10. M. I. Manning and P. C. Rowlands, *Br. Corr. J.* **15**, 184 (1980).
11. F. S. Pettit, *Trans. AIME* **239**, 1296 (1967).
12. G. R. Wallwork, *Rep. Prog. Phys.* **39**, 401 (1976).
13. J. G. Fountain, F. A. Golightly, F. H. Stott, and G. C. Wood, *Oxid. Met.* **10**, 341 (1976).
14. I. M. Allam, H. C. Akuezue, and D. P. Whittle, *Oxid. Met.* **14**, 517 (1980).